INFECTION AND IMMUNITY, Nov. 2009, p. 5190–5201 Vol. 77, No. 11
0019-9567/09/$12.00 doi:10.1128/IAI.00420-09

Streptolysin S Inhibits Neutrophil Recruitment during the Early Stages of *Streptococcus pyogenes* Infection▽†

Ada Lin,[1] Jennifer A. Loughman,[3]‡ Bernd H. Zinselmeyer,[2] Mark J. Miller,[2]* and Michael G. Caparon[3]*

Department of Pediatrics,[1] Department of Pathology and Immunology,[2] and Department of Molecular Microbiology,[3] Washington University School of Medicine, Saint Louis, Missouri 63110-1093

Received 15 April 2009/Returned for modification 24 May 2009/Accepted 10 August 2009

In contrast to infection of superficial tissues, *Streptococcus pyogenes* infection of deeper tissue can be associated with a significantly diminished inflammatory response, suggesting that this bacterium has the ability to both promote and suppress inflammation. To examine this, we analyzed the behavior of an *S. pyogenes* mutant deficient in expression of the cytolytic toxin streptolysin S (SLS$^-$) and evaluated events that occur during the first few hours of infection by using several models including injection of zebrafish (adults, larvae, and embryos), a transepithelial polymorphonuclear leukocyte (PMN) migration assay, and two-photon microscopy of mice in vivo. In contrast to wild-type *S. pyogenes*, the SLS$^-$ mutant was associated with the robust recruitment of neutrophils and significantly reduced lethal myositis in adult zebrafish. Similarly, the mutant was attenuated in embryos in its ability to cause lethality. Infection of larva muscle allowed an analysis of inflammation in real time, which revealed that the mutant had recruited PMNs to the infection site. Analysis of transepithelial migration in vitro suggested that SLS inhibited the host cells' production of signals chemotactic for neutrophils, which contrasted with the proinflammatory effect of an unrelated cytolytic toxin, streptolysin O. Using two-photon microscopy of mice in vivo, we showed that the extravasation of neutrophils during infection with SLS$^-$ mutant bacteria was significantly accelerated compared to infection with wild-type *S. pyogenes*. Taken together, these data support a role for SLS in the inhibition of neutrophil recruitment during the early stages of *S. pyogenes* infection.

The initial encounter with the host poses several challenges for extracellular bacterial pathogens that cause acute self-limiting diseases. For example, the bacterium must first establish a niche on the mucosal epithelium, which will likely require it to out-compete the resident flora. Once established, the bacterium must multiply, often to high numbers, while at the same time avoiding the host's attempt at immune clearance. The ultimate goal of the pathogen is to maximize its potential for transmission to a new host or to enter into a quiescent state to persist indefinitely in the host. The ability to balance between these tasks implies that these bacteria have the ability to both promote and suppress host responses at various stages of the infection.

Insight into the stage-specific contributions of pro- versus anti-inflammatory virulence factors will be important for understanding the pathogenesis of the myriad diseases caused by *Streptococcus pyogenes* (group A streptococcus). This gram-positive bacterium causes diseases of soft tissue that most frequently involve the more superficial layers of tissue (impetigo, pharyngitis, erysipelas, and cellulitis), but it can also sometimes be highly destructive of fascia, adipose tissue, and muscle and be associated with high rates of morbidity and mortality (necrotizing fasciitis and myositis). As a general rule, the late stages of all these diseases are characterized by robust inflammation (6, 14). However, a distinct absence of inflammation is not an uncommon presentation for advanced necrotizing fasciitis (32), and a deficiency of polymorphonuclear leukocytes (PMNs) upon histopathological examination of infected tissues is associated with a significantly increased risk of mortality from this disease (1). Thus, *S. pyogenes* appears to have the capacity to both suppress and stimulate inflammation, and the balance between these activities may be influenced by strain differences and/or stage- and tissue-specific cues in a manner that can affect the outcome of infection.

Unfortunately, understanding the contribution of many pro- or anti-inflammatory factors to a specific stage of any *S. pyogenes* disease has typically been problematic. A prominent example is streptolysin S (SLS), a potent cytolysin that has been reported to possess both proinflammatory (26) and anti-inflammatory activities (35, 53, 57) and whose contribution to virulence in a number of animal models of *S. pyogenes* disease has been the subject of several conflicting reports (for a review, see references 25 and 75). A difficulty in studying SLS has been its intrinsic instability, which has made its biochemical characterization difficult. However, analysis of SLS stabilized in complex with various carrier molecules has suggested that it is composed of a peptide with a molecular mass of approximately

* Corresponding author. Mailing address for M. J. Miller: Department of Pathology and Immunology, Washington University School of Medicine, 660 S. Euclid Ave., Box 8118, Saint Louis, MO 63110-1093. Phone: (314) 362-3044. Fax: (314) 362-4096. E-mail: miller@pathology.wustl.edu. Mailing address for M. G. Caparon: Department of Molecular Microbiology, Washington University School of Medicine, 660 S. Euclid Ave., Box 8230, Saint Louis, MO 63110-1093. Phone: (314) 362-1485. Fax: (314) 362-3203. E-mail: caparon@borcim.wustl.edu.

‡ Present address: Department of Pediatrics, Washington University School of Medicine, 660 S. Euclid Ave., Box 8208, Saint Louis, MO 63110-1093.

† Supplemental material for this article may be found at http://iai.asm.org/.

▽ Published ahead of print on 17 August 2009.

2.8 kDa (2). Consistent with this, a nine-gene operon resembling the gene clusters that encode bacteriocin-like antimicrobial peptides has been shown to be both necessary and sufficient for production of SLS (reviewed in reference 55). Similar to several other bacteriocin operons, the first gene in the SLS operon (*sagA*) encodes a protein with a predicted double-glycine signal sequence followed by a 30-amino-acid mature region that is likely secreted while the remaining genes (*sagB* to *sagI*) encode proteins for posttranslational modification, membrane transport, and an immunity factor (55). Modification likely involves heterocycle formation catalyzed by SagBCD (44). While SLS is normally nonantigenic, the observation that antibodies raised against a synthetic peptide that corresponds to the predicted SagA mature region can neutralize the cytolytic activity of SLS has provided additional evidence to support a bacterocin peptide-like nature for SLS (15).

Membrane damage associated with SLS cytotoxicity occurs via the introduction of small pores (7, 28), and almost any eukaryotic cell type is susceptible (29). The cytotoxin is rapidly lethal when injected into rabbits, causing intravascular hemolysis and cardiac abnormalities (29). However, despite this impressive toxicity, analyses of mutants engineered to be phenotypically SLS-deficient (SLS^-) have not yielded a definitive answer on the role of SLS in pathogenesis or its importance to the disease process. For example, several studies in murine models of lethal infection have found that SLS mutants are only modestly attenuated under conditions where death is a consequence of systemic dissemination (24, 67). In contrast, other studies that have analyzed the ability of SLS mutants to form local ulcerative lesions in murine subcutaneous tissue have generally observed a higher degree of attenuation (3, 17, 24), suggesting that SLS may act to promote local growth of *S. pyogenes* in tissue. In these latter studies, attenuation was associated with markedly less inflammatory tissue damage than wild-type infection, suggesting that SLS is proinflammatory. However, an anti-inflammatory effect early in infection could also lead to a subsequent reduction in tissue damage at latter time points since the mutant would be more rapidly cleared in the absence of the ability to block inflammatory cell recruitment. Thus, whether attenuation results from the loss of pro- or anti-inflammatory activities contributed by SLS is not clear.

Greater insight into the contribution of SLS to pathogenesis will require a more detailed characterization of its influence on the inflammatory response during the first few hours of infection. In the present study, we analyzed the behavior of an SLS^- mutant in several models that are well suited for the examination of the first few hours of infection, including infection of adult, embryo, and larval zebrafish; in vitro transepithelial PMN migration; and two-photon intravital microscopy of infected murine soft tissue. Taken together, these studies support a role for SLS in suppressing PMN migration to the sites of streptococcal infection during the early period of infection, and this function is independent of the lytic activity of SLS but likely dependent on an ability to inhibit the production of chemotactic signals by local host cells. The inhibition of PMN recruitment soon after infection might serve as an important immune escape mechanism in streptococcal pathogenesis.

MATERIALS AND METHODS

Strains, media, and culture conditions. Molecular cloning experiments used *Escherichia coli* Top Ten (Invitrogen), and experiments with *S. pyogenes* used wild-type strains HSC5 (30) and JRS4 (66). Strain ΩEmm is an M protein-deficient mutant derived from HSC5 (10), and SLO1 is a streptolysin O (SLO)-deficient mutant derived from JRS4 (65). Routine culture of *S. pyogenes* employed Bacto Todd-Hewitt medium (Becton-Dickinson) supplemented with 0.2% BBL yeast extract (Becton-Dickinson) (THY medium) in sealed tubes without agitation. For infection of animals, THY medium was supplemented with 2% (wt/vol) Bacto Proteose Peptone 3 (Becton-Dickinson) (TP medium). To produce solid medium, Bacto agar (Becton-Dickinson) was added to THY medium to a final concentration of 1.4%, and unless otherwise indicated, all solid cultures were incubated under anaerobic conditions produced using a commercial gas generator (BBL GasPak; catalog no. 70304; Becton-Dickinson). When appropriate, spectinomycin was added to the medium at 100 mg/ml for both *E. coli* and *S. pyogenes.* (See strain table in supplementary material.)

DNA techniques. Plasmid DNA was isolated by standard techniques and was used to transform *E. coli* by the method of Kushner (41) and to transform *S. pyogenes* by electroporation as previously described (5). Restriction endonucleases, ligases, kinases, and polymerases were used according to the manufacturers' recommendations. Chromosomal DNA was purified from *S. pyogenes* as previously described (5). The fidelity of all DNA molecules generated by PCR was confirmed by DNA sequence analyses performed by an outside vendor (SeqWright, Houston, TX).

Insertional inactivation of *sagH*. Based on prior reports (17, 56), an SLS^- mutant was constructed by insertional disruption of *sagH* (Spy0745) (23) by methods described elsewhere (48). Briefly, primers sagHdisruption up (AAA CGC GGA TCC GAT GAT CGT TAT TTT AAG TTT TGC C) and sagHdisruption down (AAA CGC GAG CTC CCC ATT TAA TAG GAG ATA TAT TCG AC) were used to amplify a 928-bp fragment within *sagH* from HSC5 chromosomal DNA. Subsequent insertion of the fragment between the BamHI and SstI of the integrational plasmid pSPC18 (49) using the sites embedded in the primers (underlined) generated the plasmid pATL28. Integration of pATL28 into the HSC5 chromosome via homologous recombination produced strain ΩSagH (SLS^-). The chromosomal structure of this mutant was verified by PCR using the appropriate primers: sagH check up (GC CAG ATT TAA TAG GAG ATA TAT TCG AC) and sagH check down (GCG CTT TAT CTT AAC AAA TAG AG). (See primer table in supplementary material.)

Phenotypic characterization of ΩSagH (SLS^-). The SLS-dependent hemolysis of the wild-type strain and ΩSagH was confirmed as described previously (58). As expected, ΩSagH did not produce detectable levels of SLS-dependent hemolysis of erythrocytes (data not shown). The growth rates of wild-type and ΩSagH were compared at both 37°C and 30°C as follows. Cultures were initiated from overnight growth in THY medium of cells that had been washed once with an equal volume of phosphate-buffered saline (PBS) (pH 7.4) to obtain an initial optical density at 600 nm (OD_{600}) of 0.01. Growth was monitored as the change in OD_{600} over time. The ability of all streptococcal strains to adhere to keratinoctyes was routinely monitored as described previously (73). A hemolysis assay for detection of SLO activity was performed as described previously (65). The presence of M protein was analyzed by Western blotting. Compared to its wild-type parent strain, ΩSagH demonstrated no growth or adherence defects or deficiency in the expression of M protein or in SLO activity (data not shown).

All animals were maintained and all animal studies were performed at the Washington University School of Medicine using protocols approved by the Animal Studies Committee in accordance with federal regulations.

Infection of zebrafish. Outbred 6-month-old adult male zebrafish (*Danio rerio*) of the ZDR wild-type strain were obtained from a commercial breeder (Aquatica Tropicals, Plant City, FL) and used to compare the ability of wild-type and mutant streptococci to cause a fatal myositis, as described previously (54). Streptococci were cultured overnight in TP medium, diluted 1:100 in fresh medium, cultured to an OD_{600} of 0.300 at 37°C, and briefly sonicated to disrupt the streptococcal chains. Groups of 10 zebrafish each were then injected with 10^5 CFU in a volume of 10 μl or with an equivalent volume of sterile TP medium in the case of mock infection. Survival was monitored for 5 days, and any differences in survival between groups infected with wild-type or mutant strains were tested for significance as described previously (54). Data presented are from a representative of three independent experiments.

Embryos were derived from wild-type ZDR zebrafish by natural mating and were maintained in embryo medium (76) for 18 h postfertilization and then moved to 0.003% phenyl-thiourea in embryo medium to prevent melanization (76). At 32 h postfertilization, embryos were dechorionated, as described previously (76), immediately prior to infection. Groups of 15 embryos each were then

injected (FemtoJet; Eppendorf) in the yolk sac essentially as described previously (18, 76) with approximately 10^3 CFU of streptococci (in 1.0 μl) that were prepared as described above, with the exception that bacteria were resuspended in PBS. Injection doses were quantitated by serial dilution of the suspension used for inoculation and plating on THY plates. Mock injection was with an equivalent volume of sterile PBS. Embryos were examined by microscopy every 2 h for the loss of viability and were considered deceased on the basis of these criteria: (i) an absence of any visible ventricular contraction upon examination of the heart and (ii) conversion from a transparent to an opaque appearance. Any deaths that occurred within 2 h postinjection were attributed to injection trauma and were excluded from the study. Any differences in survival between the wild type and mutant were analyzed for significance as described for infection of adult fish.

Larvae derived from the pu.1 transgenic line (36) by natural mating were raised by standard methods (76) and were maintained in embryo medium for up to 7 days postfertilization. Streptococci were intrinsically labeled with CellTracker Orange ([CTO] catalog number C-2927; Molecular Probes) as follows. Bacterial strains were cultured as described earlier, harvested by centrifugation, and then resuspended in prewarmed PBS containing 0.015 mM CTO. Following a 30-min incubation at 37°C, the labeled streptococci were harvested by centrifugation and resuspended in prewarmed TB medium. After an additional 30-min incubation at 37°C, streptococci were washed twice in PBS and then resuspended in PBS. This treatment had no effect on streptococcal viability as assessed on the basis of growth rates (data not shown). Larvae were then injected under tricaine anesthesia (0.25 mg/ml) at the midline of the dorsal muscle immediately anterior to the dorsal fin with approximately 10^3 CFU of streptococci.

Quantification of PMNs. Infected adult zebrafish (three per group) were euthanized with tricaine (0.5 mg/ml) at 3-h intervals up to 48 h postinfection and immersed in fixative (Histochoice; Sigma). Tissues were then paraffin embedded and stained with hematoxylin-eosin by standard methods. PMNs were identified based on their characteristic multilobed nuclei. Infected larvae were examined every 2 h by fluorescence microscopy (Leica model DMIRE2) and observed for fluorescence using both the green fluorescent protein ([GFP] PMNs) and rhodamine filters (bacteria). PMNs were identified by their green fluorescence. The number of PMNs in tissue was then assessed as described by Klein et al. (40). Images were captured using a QImaging Retiga 1350 EX charged-coupled-device camera and OpenLab software (Improvision) and processed for publication using Canvas X (ACD Systems).

Bacterial quantification. In selected experiments, groups of three adults or five embryos each were euthanized with tricaine every 6 h up to 24 h postinfection. The numbers of bacterial CFU for adults were determined as previously described (69). Bacterial load in embryos was determined as previously described (71).

Injection and imaging of mice. Female adult LysM-eGFP mice, were obtained from Klaus Ley (Robert M. Berne Cardiovascular Research Center, University of Virginia) who backcrossed the originally generated mice from T. Graf (Albert Einstein College of Medicine, Bronx, NY) to the B6 background (22). C57BL6 LysM-eGFP mice in which neutrophils and macrophages express the enhanced GFP (eGFP) were injected in the footpad with 1×10^8 CFU of *S. pyogenes*, either the wild-type or SLS^- strain, in ~5 μl of PBS. During the imaging process, mice were anesthetized with isofluorane for restraint and to avoid psychological stress on the animal. VetBond (3 M) was used to secure the paw to the glass coverslip at the bottom of the imaging chamber, and PBS was added to cover the tissue. The mouse's core body temperature was maintained with a warming pad (Braintree Scientific) set to 37°C. To label blood vessels during imaging, 1 mg of dextran tetramethylrhodamine (molecular weight of 2,000,000; Invitrogen), was injected by intravenous or retro-orbital route. The rear footpad and toes were imaged for a period of 1 h before the mouse was euthanized while deeply anesthetized. Time-lapse imaging was performed using a custom-built dual laser video-rate 2P microscope. GFP-labeled neutrophils and rhodamine dextran-labeled blood vessels were excited by a Chameleion XR Ti:sapphire laser (Coherent) tuned to 820 nm. Fluorescence emission was passed through 490-nm and 560-nm dichroic mirrors placed in series and detected as red (560 to 650 nm), green (490 to 560 nm), and blue (<490 nm) channels by three head-on bialkali photomultiplier tubes. A customized version of ImageWarp (A&B Software) was used to control the various hardware devices during real-time acquisition and to process and archive the image data. Each plane consists of an image of 200 mm by 225 mm (*x* and *y*, 2 pixel/mm). Z-stacks were acquired by taking 31 sequential steps at 2.5-mm spacing. To increase signal contrast, we averaged 15 video frames for each slice with a 5-s delay between steps. Multidimensional rendering was performed with Imaris (Bitplane), and cell tracking was performed with PicViewer software (John Dempster, University of Strathclyde) (77).

Neutrophil tracking. Neutrophils were identified by their characteristic shape and movements and their fluorescence, which is brighter than that of macrophages/monocytes, as previously described (22, 78). Neutrophils were classified as either inside or outside of vessels based on their colocalization with intravenously injected rhodamine dextran and on their characteristic flow and rolling behavior. Neutrophil migration in the connective tissue was tracked by measuring the cell's center of mass. Cell velocity was calculated on a cell track basis and reported as median velocity ± standard error of the mean. The cell's meandering index was obtained by dividing the cell's displacement from the origin (after 5 min) by the track length. Values above 0.75 indicate highly directional migration, consistent with chemotactic behavior.

Human PMN isolation. Neutrophils were isolated from the venous blood of healthy volunteers using dextran sedimentation, followed by Ficoll density gradient centrifugation and hypotonic lysis of contaminating red blood cells as described previously (61). PMN viability was greater than 95% as assessed by trypan blue exclusion and greater than 95% pure as determined by visualization of nuclear morphology after staining (Hema 3; Fischer Scientific). For migration assays, cells were resuspended in prewarmed chemotaxis medium (see below) at a concentration of 10^7 cells/ml and used immediately.

Preparation of inverted epithelial layers. The HaCaT human keratinocyte cell line (4) was cultured as described previously (73) in Dulbecco's modified Eagle's medium with 8 mM L-glutamine, 25 mM HEPES, and 5% (vol/vol) fetal calf serum (all final concentrations). Trypsinized cells were resuspended to a concentration of 3×10^6 cells/ml, and 50 μl of the suspension was seeded on inverted Transwell inserts (0.33-cm^2 polycarbonate membranes with 3-μm diameter pores; catalog number 3472; Corning). The cells were allowed to attach to the membranes in a humidified 5% CO_2 atmosphere at 37°C for 16 h and were then transferred to 24-well plates with 0.6 ml of fresh medium in each well, and 0.2 ml of medium was added to the basolateral chamber. After 10 to 11 days of incubation with medium refreshed every 2 days, confluent cell layers were obtained. The electrical resistance of confluent monolayers was not detectable by traditional methods; therefore, monolayer integrity was determined by assessing the permeability to fluid as described previously (47). A monolayer was accepted as polarized if the basolateral chamber remained completely full of medium and did not equilibrate with the apical chamber after an overnight incubation.

PMN transepithelial migration assay. At the beginning of each experiment, inverted HaCaT monolayers were washed three times with chemotaxis medium, which consists of the HaCaT medium described above prepared without serum and phenol red. Overnight cultures of bacteria grown in THY broth were washed once in PBS and suspended in chemotaxis medium at a concentration of 10^8 CFU/ml. Transwell inserts were lifted from each well and placed in a moist chamber with the cell layer facing up. An aliquot of the bacterial suspension (25 μl) or an equivalent volume of sterile medium was placed on top of the epithelial layers (a multiplicity of approximately 10 CFU/cell) and incubated for 60 min at 37°C. Nonadherent bacteria were removed by immersing the inserts three times in culture trays containing chemotaxis medium. The cell layers were inverted and transferred into new 24-well culture plates (Ultra Low attachment plates; Corning catalog number 3473) containing 0.6 ml of chemotaxis medium. An aliquot of the PMN suspension (10^6 cells) was then added to the basolateral chamber, and following a 60-min incubation at 37°C, the contents of the apical chamber were mixed by gentle pipetting and then transferred to a centrifuge tube. To quantify transepithelial migration of PMNs, an aliquot of this suspension was examined by microscopy, and the number of PMNs was enumerated using a hemocytometer. The number of PMNs recruited by each mutant is shown as a percentage of the number recruited by the wild-type strain, and the data presented represent the mean and standard deviation of the mean derived from at least three independent experiments, with samples analyzed in triplicate. For the interleukin-8 (IL-8) assay, 100 μl of chemotaxis medium was added to the basolateral chamber, and 600 μl of chemotaxis medium was present in the apical chamber. After a 1-h incubation at 37°C, tissue culture supernatants from both chambers were collected and evaluated for IL-8 using an IL-8 Singleplex assay according to the manufacturer's instructions (Bio-Rad Laboratories, Hercules, CA). The results represent the mean and standard deviation of the mean from three independent experiments with 10 replicates for each sample.

Production of ROS. The production of reactive oxygen species (ROS) by human PMNs was measured using a kinetic assay for fluorescence of an indicator compound, 2′,7′-dihydrodichlorofluorescein diacetate (catalog number C2938; Molecular Probes). Purified human PMNs were incubated with a 10 μM concentration of the reagent for 30 min at room temperature in PBS. The treated PMNs (10^6 cells) were used in a transepithelial migration assay performed as described earlier with the following modifications. The HaCaT cells were grown on permeable cell culture inserts that block transmission of light such that independent fluorescence signal measurements can be taken from the top and

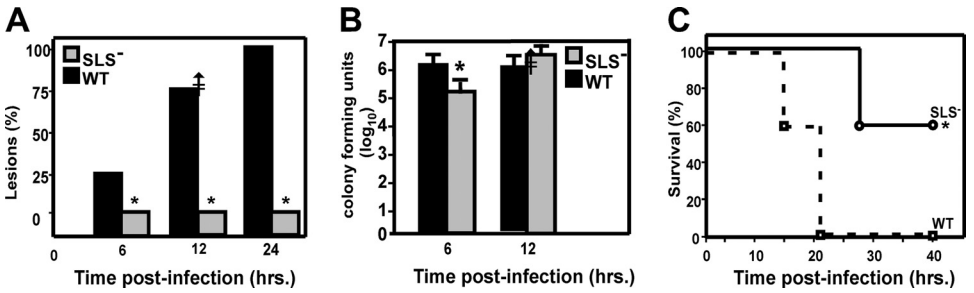

FIG. 1. The SLS$^-$ mutant is attenuated in the adult zebrafish model of necrotic myositis. Groups of zebrafish were challenged intramuscularly with 10^5 CFU of mutant (SLS$^-$) or wild-type (WT) *S. pyogenes.* Significant differences are indicated by an asterisk. (A) Percentage of fish with lesions at 6, 12, and 24 h. The data represent the average of 10 fish per experiment over three separate experiments at the indicated time points. There were significantly fewer lesions ($P < 0.02$) in the mutant group at each time point. (B) Numbers of CFU recovered from infected tissue at 6 and 12 h. Data represent the mean and standard deviation of three separate experiments. A significant difference was seen at 6 h but not at 12 h. (C) Survival data presented as a Kaplan-Meier plot. Data are pooled from three independent experiments, each of which was conducted using 10 zebrafish per group. These data indicate that the mutant was significantly less lethal than the wild type ($P < 0.0043$).

bottom compartment in the appropriate companion plate (BD Falcon Fluoro-Blok; catalog numbers 351151 and 353504, respectively) and transferred to a heated microplate fluorometer (Synergy 2; BioTek) at the onset of the migration experiment. It was determined that HaCaT cell growth and PMN transepithelial migration under these conditions were similar to results with the standard assay. The amount of ROS generated in the bottom compartment was measured for 120 min at 37°C using excitation and emission wavelengths of 485 and 528 nm, respectively, and normalized to the number of PMNs migrated. Data are relative fluorescent units per 10^4 PMNs and represent the mean and standard deviation of five samples.

PMN apoptosis. The ability of *S. pyogenes* to induce PMNs to undergo apoptosis was measured as follows. Bacterial and PMN suspensions were prepared in chemotaxis medium as described for the transepithelial migration assay above and combined at a ratio of approximately 10 CFU/cell. Samples were transferred to a 37°C incubator with 5% CO_2 for 60 or 120 min prior to analysis. Control PMNs were incubated with medium in the absence of bacteria. Apoptosis was evaluated by determination of the number of PMNs that demonstrated surface localization of phosphatidylserine as revealed by staining with annexin V conjugated to the fluorochrome phycoerythrin (PE). Staining used a commercial kit (catalog number 559763; BD Biosciences) and was conducted according to the protocol provided by the manufacturer. Fluorescence of individual cells was measured using a flow cytometer (FACSCalibur; Beckman-Coulter), and mean fluorescence values were determined from a minimum of 5×10^4 cells within an analysis region corresponding to the nonfragmented neutrophils identified using Cell Quest software (BD Biosciences). The number of apoptotic cells in samples incubated with bacteria is shown as a ratio relative to the number of annexin V-PE-positive cells in uninfected control samples and reflects the mean and standard deviation of two independent experiments, each of which was analyzed in duplicate.

Statistical analyses. Data were analyzed as means ± 1 standard deviation from the mean. Kaplan-Meier product limit estimates of survival curves were used to compare infection by wild-type and mutant streptococci, and any differences in survival were tested for significance as described previously (54). Where noted, the significance of differences observed between experimental groups in other assays was evaluated using a Student's *t* test. Extravasation kinetics were compared using both Pearson (parametric) and Spearman (nonparametric) correlations. Median track velocities and the meandering index were compared by a Mann-Whitney test. *P* values of less than 0.05 were considered statistically significant.

RESULTS

SLS$^-$ mutants are attenuated in the zebrafish model of necrotic myositis. Inactivation of any gene in the SLS operon produces a mutant that is phenotypically defective in production of detectable SLS (56). Based on this, we generated an insertion mutation in *sagH* in wild-type strain HSC5, whose virulence has been extensively characterized in the zebrafish model of necrotic myositis that reproduces several features commonly observed in *S. pyogenes* infection of human muscle (54). The virulence of this mutant was then compared to its wild-type parent for its ability to cause disease in zebrafish. Both streptococcal strains were inoculated into the dorsal muscle of zebrafish at a dose approximately 10-fold the 50% lethal dose for the wild-type strain. After 12 h, a significant majority of the zebrafish infected with the mutant (SLS$^-$) failed to form the expected pale lesions, as seen in wild-type infections ($P < 0.02$) (Fig. 1A). Also, at 12 h after infection, most of the zebrafish in both infection groups remained viable (Fig. 1C), and both the wild-type and the SLS$^-$ mutant had multiplied to similar extents in muscle tissue even though in the first 6 h SLS$^-$ bacteria grew at a slightly slower rate (Fig. 1B). However, it is important that the magnitude of this difference, while statistically significant, is not striking (less than a 1-log difference, with overall burdens between 10^5 to 10^6 CFU), so the proliferative ability of both strains was essentially the same. Following this initial period, greater than 90% of zebrafish infected with the wild type did not survive beyond day 2 (Fig. 1C). In contrast, greater than 60% of zebrafish infected with the mutant were still viable at 40 h postinfection (Fig. 1C), demonstrating that the loss of SLS rendered *S. pyogenes* significantly less virulent ($P < 0.0043$).

Infection by the SLS$^-$ mutant promotes an elevated PMN infiltrate. To determine the basis for the longer viability of zebrafish infected by the mutant, histological analyses were conducted on infected tissues recovered at 3-h intervals over a 48-h period. By 6 h the wild-type strain had produced the characteristic extensive necrosis associated with large numbers of extracellular streptococci, based on dissections along planes of remnant tissue (Fig. 2A) (see also reference 54). SLS$^-$ mutant-infected tissue showed reduced necrosis, few visible streptococci (Fig. 2B), and a vigorous infiltrate of PMNs ($P < 0.001$) (Fig. 2C). Thus, as reported for the murine model (3, 17, 31, 50, 64), the attenuation of the SLS$^-$ mutant was associated with a more robust inflammatory response.

***S. pyogenes* SLS$^-$ mutant is attenuated for virulence in zebrafish embryos compared to the wild type.** Zebrafish embryos have been used to study the behavior of phagocytes during inflammation (31, 50, 64) and to study early events in the interaction between phagocytic cells and several facultative

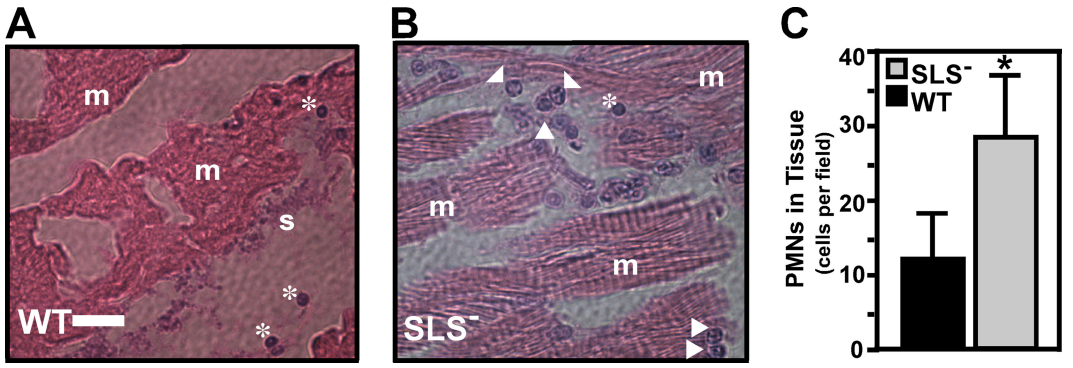

FIG. 2. Infection by the SLS$^-$ mutant demonstrates a neutrophil-rich infiltrate. Adult zebrafish were infected in the dorsal muscle by either the wild type (WT) or the SLS$^-$ mutant, as indicated. Zebrafish from each infection group were fixed in toto. Longitudinal sections (5 μm thick) were stained with hematoxylin and eosin, and then the area of injection/infection was examined by microscopy. The panels show samples from 6 h postinfection with the wild-type strain HSC5 (A) and the SLS$^-$ strain ΩSagH (B). Features apparent in the micrographs are denoted as follows: arrowheads, PMNs; asterisks, erythrocytes; m, striated muscle; and s, streptococci. The bar in the left panel represents 30 μm, and the center panel is shown at the same magnification. (C) Numbers of PMNs that infiltrated infected tissue as determined by microscopic examination of stained sections by blinded observers. Data represent the mean and standard deviation of the number of individual PMNs observed per microscopic field and are pooled from sections prepared from three infected zebrafish per experimental group. There were significantly more PMNs observed in tissue infected by the SLS$^-$ mutant ($P < 0.001$).

intracellular pathogens, including *Mycobacterium* (18) and *Salmonella* (71). Based on these studies, we used microinjection to introduce *S. pyogenes* into yolk sacs of embryos that were at least 32 h postfertilization (Fig. 3A), reasoning that this would require migration of inflammatory cells to the site as with streptococcal deep-tissue infection. In our experiments, approximately 10^5 CFU of *S. pyogenes* delivered to the yolk sac was lethal to >90% of embryos by 24 h, while at this time point nearly all embryos remained viable with a similar dose of an SLS$^-$ strain (Fig. 3B), as did embryos injected with sterile PBS (Fig. 3B). Overall, a comparison of wild-type and mutant virulence revealed that the mean time to death was significantly shorter for wild-type infection than for infection with the mutant ($P < 0.01$). Infected embryos were sacrificed every 30 min for up to 6 h postinfection, and the number of CFU was then determined in homogenates. This analysis revealed that, similar to results of the adult study, both the mutant and wild-type strains multiplied to similar extents (Fig. 3C) over time, which is consistent with analysis of in vitro growth curves at 30°C, the temperature for zebrafish culture and infection (data not shown); thus differences in strain survival are not the primary explanation for the attenuated virulence, and this suggests that a host factor may be involved.

SLS$^-$ mutant bacteria induce increased PMN recruitment in larvae. The observation that infection with the mutant was associated with enhanced PMN recruitment in adult fish suggested that PMN responses might also be an important host factor limiting virulence in embryos. To test this, we injected mutant and wild-type *S. pyogenes* into the well-developed dorsal muscle of transgenic pu.1 larvae (7 days postfertilization) in which the myeloid lineage has previously been shown to expresses GFP fluorescence that correlates with immunohistochemistry staining for myeloid cells (36, 64, 74). The streptococci were intrinsically labeled with a fluorescent dye (CellTracker Orange) and were readily visible in muscle when infected larvae were examined by fluorescent microscopy (using CTO) (Fig. 4C and D). In larvae infected with wild-type bacteria for 2 h, only a modest accumulation of GFP-positive cells was observed at the site of infection (Fig. 4E). In contrast, infection with SLS$^-$ mutant bacteria led to a striking accumulation of GFP-positive cells (Fig. 4F). Furthermore, this accumulation overlapped with the location of the mutant in the muscle (Fig. 4H). As with results in the adult model, significantly higher numbers of PMNs were observed to have infiltrated to the site of infection by the mutant ($P < 0.0001$) (Fig. 4I).

SLS$^-$ alters epithelial cell signaling in a transepithelial PMN migration assay. The zebrafish infection experiments suggest that SLS is involved in reducing the number of PMNs present at the site of streptococcal multiplication. This could be due to the ability of SLS to kill PMNs (28, 35, 53) or to an effect on local host cells that inhibits their ability to express chemotactic alarm molecules. To distinguish between these possibilities, we adapted an in vitro transepithelial PMN migration assay that has been used to assess how the interactions between several pathogens and a polarized epithelium can lead to the recruitment of PMNs (reviewed in reference 51). In addition, the use of a polarized epithelium presents the epithelial cells in a more physiological context and monitors PMN migration in the more relevant basolateral-to-apical direction (51). For the current analysis, human keratinocytes were employed because of their relevance to streptococcal infection and because it has been shown that *S. pyogenes* binds to nonpolarized human keratinocytes and promotes a proinflammatory response, characterized by enhanced expression of several cytokines, and a more rapid release of prostaglandin E_2 (65, 73). The HaCaT human keratinocyte cell line was used to generate polarized monolayers on inverted permeable filter supports, and then their apical surfaces were infected with *S. pyogenes*. Subsequently, freshly isolated human PMNs were exposed to the basolateral surface of the monolayer, and the number of PMNs recruited to the apical surface was determined 1 h after infection. Upon the addition of 1×10^6 PMNs, infection by the wild-type strain HSC5 resulted in recruitment of approximately 25% of these PMNs (Fig. 5, left panel) and approximately 46% for an unrelated wild-type strain, JRS4

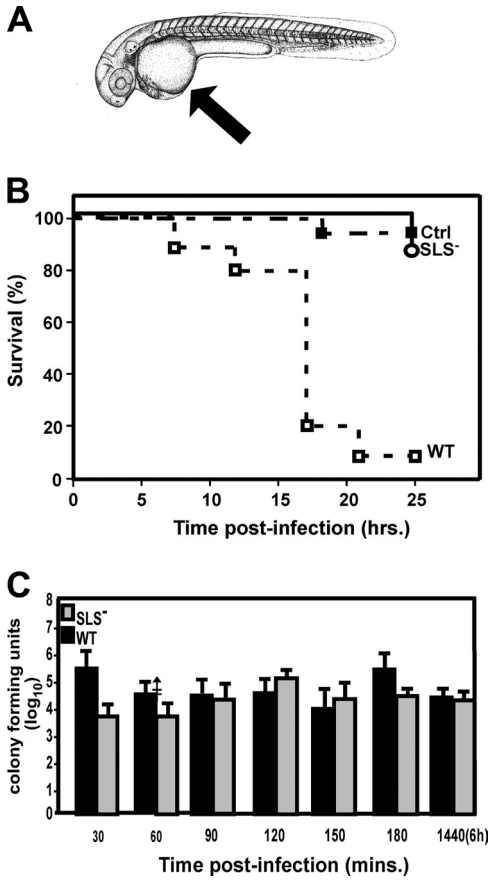

FIG. 3. *S. pyogenes* is virulent in zebrafish embryos but, as in adult zebrafish, the SLS$^-$ mutant is not as virulent. (A) Yolk sac injections. The site of injection of 1×10^5 CFU of wild-type (WT) *S. pyogenes*, the SLS$^-$ mutant, or PBS alone (Ctrl) in the yolk sac is indicated by the arrow. The diagram was adapted from Kimmel et al. (39) with permission of the publisher, John Wiley & Sons, Inc. (B) Analysis of virulence. The survival data of injected embryos are presented as a Kaplan-Meier plot. Infected embryos were examined for viability every 2 h by microscopy. Data shown are pooled from three independent experiments using 15 embryos per group. These data show that the SLS$^-$ mutant is significantly attenuated ($P < 0.011$). (C) Infected embryos were sacrificed every 30 min during the first 6 h of infection for assessment of the number of CFU. Groups of five embryos each were examined at each time point for each strain analyzed. The data shown represent the mean and standard deviation of three independent experiments. There was no significant difference between groups.

(Fig. 5, right panel). Furthermore, efficient recruitment required the presence of keratinocytes (Fig. 5, compare results for the wild type with and without keratinocytes in the left panel), suggesting that host-pathogen interactions at the apical keratinocyte surface were generating chemotactic signals released to the basolateral membrane. Supporting this was the observation that an M protein-deficient mutant, which cannot adhere to keratinocytes (59), and a mutant that cannot express the proinflammatory molecule SLO (65) had reduced abilities to recruit PMNs and recruited these cells only at the levels observed in the absence of keratinocytes (Fig. 5). In contrast, infection with the SLS$^-$ mutant produced a significantly greater inflammatory response than the wild-type strain ($P < 0.001$) (Fig. 5, right panel), and this response was more than fourfold greater than that produced by the M protein-deficient mutant (Fig. 5, left panel). Furthermore, this enhanced level of recruitment was dependent on the presence of keratinocytes (Fig. 5, compare results for the SLS$^-$ strain with and without keratinocytes). The altered pattern of migration observed over the course of the assay was likely not due to any direct effect of SLS on PMNs as greater than 95% of the PMNs recruited by either the wild-type strain or the SLS$^-$ mutant were viable (data not shown). When results were normalized for the total number of PMNs recruited, there was no significant difference in the production of ROS by PMNs during transepithelial migration (Fig. 6A), nor was there a significant difference in the ability of either streptococcal strain to promote neutrophil apoptosis (Fig. 6B) within the observed time frame.

Neutrophil extravasation is altered by SLS in a mouse model of streptococcal infection. In order to determine what step in neutrophil recruitment might be involved in the delayed presence of neutrophils at the recruitment site, we compared the recruitment kinetics of neutrophils after subcutaneous infection with wild-type and SLS$^-$ bacteria in mice using in vivo two-photon microscopy. Neutrophils were identified by their characteristic shape, movements, and fluorescence, which is brighter than that of macrophages/monocytes, as previously described (22, 78). Within minutes of infection with either the wild-type or SLS$^-$ strain, similar numbers of GFP-positive neutrophils were found rolling along the lumen of small vessels near the site of injection and adhering firmly to the surface of the endothelium (Fig. 7A; see also Movies WT and SLS$^-$ in the supplemental material). In response to inoculation with wild-type bacteria, most neutrophils remained in the vessels for tens of minutes before appreciable numbers extravasated (=time at which 50% of the imaged cells are still in the vessel, 52 min) (Fig. 7B; see also Movie WT in the supplemental material) and began to migrate through the connective tissues. In contrast, the rate of extravasation of neutrophils recruited in response to SLS$^-$ bacteria was significantly increased (time at which 50% of the imaged cells are still in the vessel, 28 min) (Fig. 7B; see also Movie SLS$^-$ in the supplemental material). Thirty-five minutes after infection with the wild type, greater than 80% of neutrophils remained in the blood vessels, whereas at the same time during SLS infection, less than 40% of the neutrophils were inside vessels. However, once neutrophils completed diapedesis, they migrated with similar velocities (Fig. 7C) and directional biases (Fig. 7D) in response to either wild-type or SLS$^-$ infection. This response is highly localized to the infection site since we saw similar results in the same mouse paw that had wild-type bacteria injected in one toe and SLS$^-$ bacteria injected into an adjacent toe. In summary, in this model, neutrophils in both types of infections appeared to be recruited similarly to the site of infection, and, once they had exited the vessel into the tissue, they also appeared to behave similarly. The rate-limiting step appears to be the difference in timing of the exodus of the neutrophils from the vessel lumen into the tissue and not their overall accumulation, which could explain the earlier appearance of PMNs in SLS$^-$ infections than in wild-type infections.

IL-8 expression was not altered between keratinocytes infected by wild-type or SLS$^-$ streptococci. Both mouse and transwell data suggest that SLS has a local effect on PMN migration that may involve alterations in chemotactic signaling

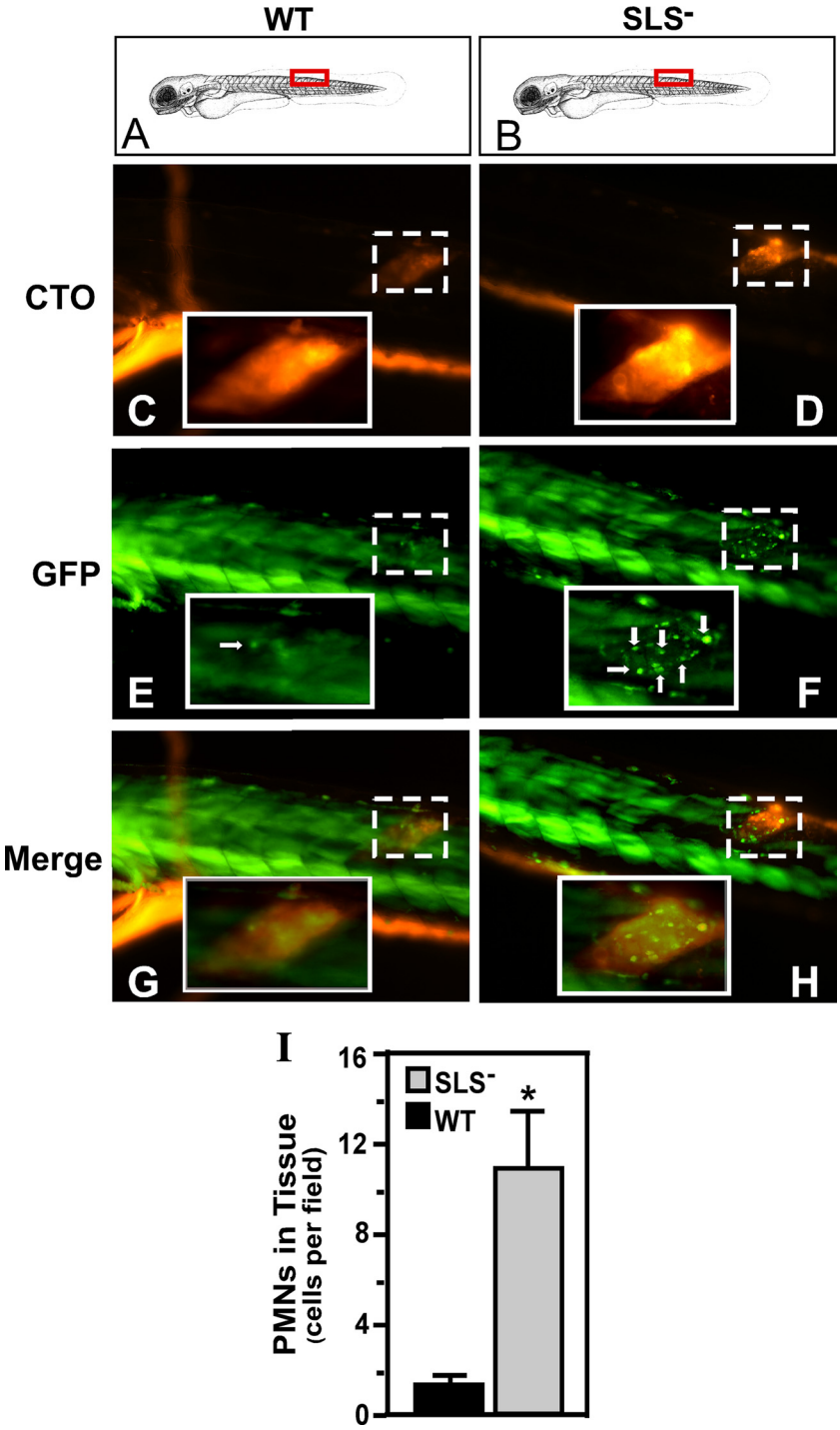

FIG. 4. The SLS$^-$ mutant also promotes a PMN-rich infiltrate in embryos. pu.1 larvae (7 days postfertilization) which express GFP fluorescence specifically in cells of the myeloid lineage were injected in the dorsal muscle with 10^3 CFU of either the wild type (WT) or the SLS$^-$ mutant intrinsically labeled with the fluorescent dye CTO at the site indicated by the red boxes in panels A and B. Infected larvae were examined by fluorescent microscopy at 2 h postinfection for CTO fluorescence (C and D and GFP fluorescence (E and F; PMNs are indicated by white arrows). As noted by Hsu et al., in the larval form, the skeletal muscle (even in wild-type-infected fish) contributes background fluorescence that is easily distinguished from individual myeloid cells (36). The columns show images taken from single representative larvae, oriented as indicated in the top panels (A and B), that were infected with the wild type (WT) or the SLS$^-$ mutant. Panels G and H show the merged images. The site of injection in each fish is demarcated in the micrographs by the boxes with the broken white line. Magnification, ×10. The insets outlined by the boxes with the unbroken white lines show the injection site at a higher magnification (×40). The diagram in panels A and B was adapted from Kimmel et al. (39) with permission of the publisher, John Wiley & Sons, Inc. (I) The number of PMNs that infiltrated the infected tissue as determined by microscopic examination by blinded observers. Data shown represent the mean and standard deviation of the number of individual PMNs observed per microscopic field and pooled from three infected zebrafish per experimental group. As with the results of infections of adults, there were significantly more PMNs observed in tissue infected by the SLS$^-$ mutant than in wild-type-infected tissue ($P < 0.0001$).

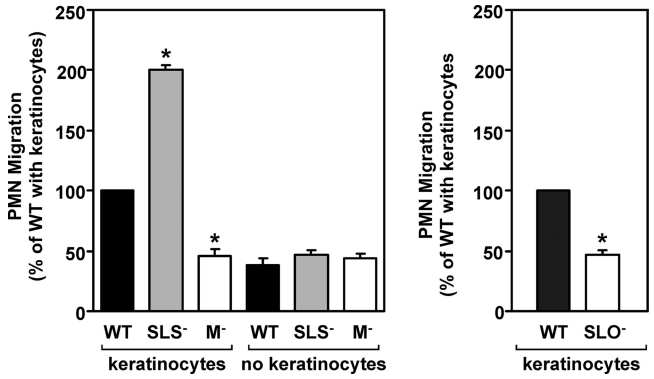

FIG. 5. Neutrophil recruitment is altered by SLS and requires the presence of keratinocytes. The number of PMNs recruited to the basolateral surface of a polarized HaCaT keratinocyte monolayer (keratinoctyes) following infection with various *S. pyogenes* strains. Monolayers were infected at their apical surfaces at 10 CFU/epithelial cell, and then 1×10^6 PMNs were added at the basolateral surface of the monolayer. The number of PMNs recruited to the apical surface was enumerated at 60 min postinfection and is shown relative to the number recruited in response to each wild-type strain. PMN recruitment in the absence of a monolayer is also shown (no keratinoctyes). In the left panel, strains derived from HSC5 (WT) include the SLS^- mutant ΩSagH and the M protein-deficient mutant ΩEmm (M^-). In the right panel, the SLO-deficient mutant SLO1 (SLO^-) was derived from JRS4 (WT). An asterisk indicates that recruitment by the indicated strain was significantly different from the wild type ($P < 0.001$) under the same conditions. Data shown represent the mean and standard deviation of the mean derived from three independent experiments.

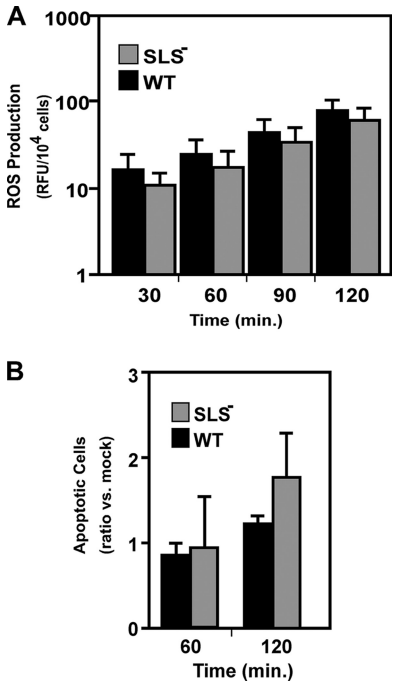

FIG. 6. Characterization of PMN exposed to *S. pyogenes* in vitro under conditions of transwell infections. (A) The ability of PMNs to produce a respiratory burst in the presence of keratinocytes infected with wild-type (WT) or SLS^- *S. pyogenes* is shown. Human PMNs loaded with an indicator dye that fluoresces in the presence of intracellular ROS were tested in the transepithelial migration assays, and the data are presented as the amount of fluorescence (relative fluorescent units [RFU]) per 10^4 migrated cells. Data represent the mean and standard deviation of six samples from two independent experiments. (B) The number of PMNs undergoing apoptosis when exposed to wild-type (WT) or SLS^- *S. pyogenes* is shown, as determined by staining with annexin V-PE. Data presented show the ratio of the number of apoptotic cells observed upon exposure to the indicated strain versus the number observed in the absence of any streptococci and represent the mean and standard deviation of two independent experiments, with samples analyzed in duplicate. Differences between mean values at each time point shown in both panels were not significant.

by adjacent host cells. The major chemotactic cytokine for PMNs known to be involved in streptococcal infection of keratinocytes is IL-8 (73), so IL-8 activity was evaluated in the apical and basolateral chambers of the transwells to see if the altered pattern of migration observed in SLS^- strains might be related to differences in IL-8 concentration. Tissue culture supernatants were collected from both chambers after 1 h of infection and analyzed for the presence of IL-8. IL-8 concentrations were similar between wild-type and mutant transwell infections. The apical chambers of both strains had significantly less IL-8 than the basolateral chambers of both strains (Fig. 8). These results demonstrate no difference in IL-8 expression levels between the two types of infection and further suggest that PMNs would be migrating against the IL-8 gradient to interact with the bacteria at the apical side of the cell since IL-8 is higher in the basolateral wells than in the apical wells in both types of infection. Furthermore, these results would imply that IL-8 is not a major contributor to neutrophil recruitment across the transwell epithelial layer and that another chemotactic agent might be involved in this effect.

DISCUSSION

Analyzing the early events in infection can present a considerable challenge due to the limitations inherent in many animal models, including the relatively low numbers of bacteria present at early time points and the difficulties associated with imaging the host response in real time in unfixed tissues. The fact that there are relatively few representative animal models for the myriad forms of streptococcal disease provides an additional complication for the study of the early elements of host-pathogen interaction for *S. pyogenes*. Our adaptation of multiple models that are particularly well suited to interrogate the first few hours of infection revealed that SLS makes an important contribution to the ability of *S. pyogenes* to manipulate the host inflammatory response during the early stages of infection.

Zebrafish embryos and larvae have numerous advantages for the study of inflammatory processes; in particular, their small size and transparency have been used to great advantage for imaging phagocyte behavior in real time using various light microscopy techniques (31) and using fluorescent microscopy in combination with transgenic lines engineered to express fluorescent proteins in cells of the myeloid lineage (36, 50, 64). Zebrafish have well-developed innate and adaptive immune systems, with the former including both Toll-like receptors that are highly conserved in mammals (37, 52) and conserved signaling pathways that include adaptor proteins such as MyD88 (72). It has been shown that inflammation is both induced and resolved over a time course similar to time courses of the more

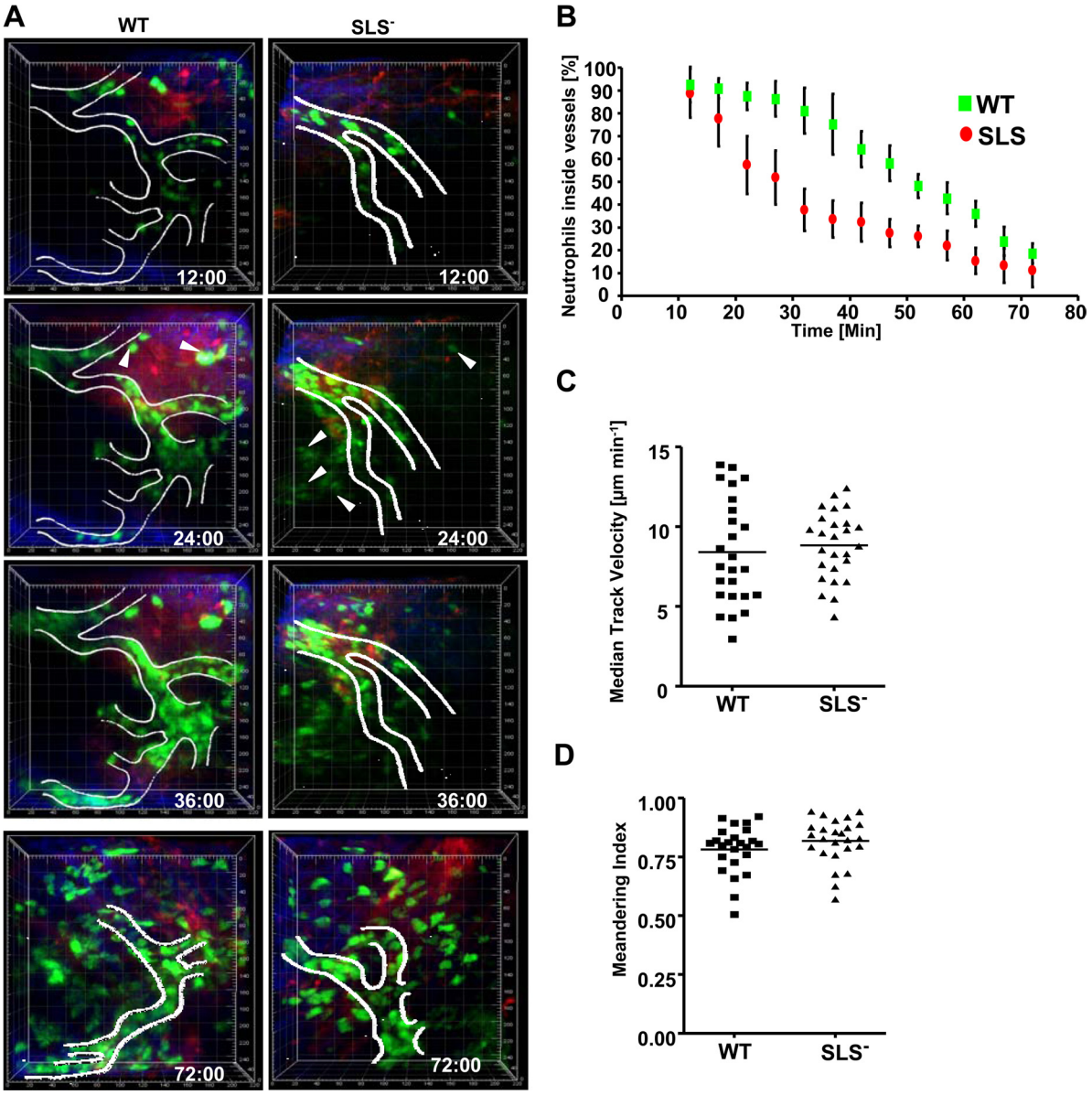

FIG. 7. In vivo imaging of neutrophil recruitment in mice infected with wild-type (WT) and SLS$^-$ streptococci. Intravital imaging was performed at the injection site on the paws of LysM-eGFP mice after subcutaneous infection with streptococci. Data were pooled from three independent experiments. (A) Representative time-lapse images of neutrophil recruitment in response to wild-type and SLS$^-$ mutant bacteria. Images are three-dimensionally rendered volumes (200 μm by 225 μm by 75 μm). Neutrophils (eGFP) appear green, collagen fibers in the connective tissue appear blue, and blood vessels (unless occluded by cells) appear red. White lines show the outline of blood vessels based on both the fluorescent-dextran signal and the characteristic flow of circulating neutrophils. White arrowheads show extravasated neutrophils at 24 min. The time stamp indicates minutes postinfection. The scale grid is labeled in micrometers. (B) The percentage ± standard deviation of neutrophils remaining in blood vessels over time in LysM-GFP mice infected with wild-type and SLS$^-$ bacteria. The curves are statistically different ($P < 0.01$) with both Pearson (parametric) and Spearman (nonparametric) correlations. (C) Interstitial neutrophil migration velocity. The plot shows the median track velocities of 25 extravasated neutrophils in wild-type and SLS$^-$ mutant infections. No statistical differences were observed. (D) The meandering index was calculated for each track in panel C. The median meandering indices of neutrophils after wild-type and SLS$^-$ mutant infection were not statistically different.

well-developed mammalian experimental systems (50, 64), and studies of PMN migration in zebrafish using real-time methodologies have revealed novel PMN behaviors such as retrograde chemotaxis (50). The present study extends the utility of using zebrafish for analysis of the early stages of infection by an extracellular bacterial pathogen, and further studies using these models should be useful for understanding how *S. pyogenes* balances the expression of its pro- and anti-inflammatory virulence factors in response to both tissue-specific and disease progression cues.

Similarly, two-photon microscopy has also been applied with great success to studying the immune system in vivo and, more recently, neutrophil recruitment during inflammation in real time (11, 62, 78). Our use of two-photon imaging supports a

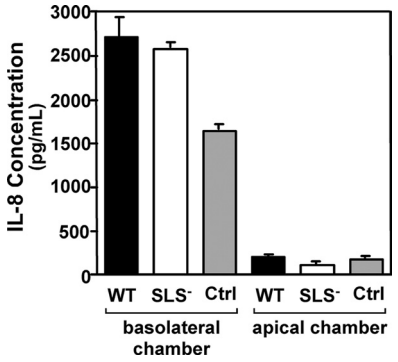

FIG. 8. IL-8 expression is similar in transwells infected with either wild-type or SLS-deficient streptococci. Polarized HaCaT keratinocyte monolayers were treated with 1×10^6 bacteria/monolayer of wild-type (WT) bacteria, an equivalent concentration of SLS$^-$ bacteria, or an equivalent volume of chemotaxis medium alone as a control (Ctrl). The monolayers were assessed for IL-8 secretion in the apical and basolateral compartments. Each strain was represented by 10 wells per experiment, and data presented are representative of an experiment performed three times.

role for SLS in acting to impede diapedesis to prevent PMN migration into infected tissue. These data suggest that the reduced virulence of SLS mutants results from a failure to inhibit neutrophil recruitment rather than via a loss of any of its reported proinflammatory activities.

While it has been well recognized that *S. pyogenes* can express numerous proinflammatory virulence factors like SLO (65) and M protein (60), it has also been noted that *S. pyogenes* can express factors capable of active suppression of inflammation. These include the cell wall-associated proteases SpcA and SpcC. The former is a subtilysin family protease that cleaves and inactivates the chemotactic C5a component of complement (12) while the latter is a serine protease that degrades CXC-type chemokines, such as IL-8, keratinocyte-derived chemokine, and MIP-2 (19, 32, 33). Mutants that cannot express these proteases have been reported to possess altered virulence in several animal models of infection (33, 38). Interestingly, as proteases, the anti-inflammatory activities of both SpcA and SpcC require them to come into direct contact with their substrates. Furthermore, both are covalently anchored to the peptidoglycan of the streptococcal cell surface by the sortase pathway (8, 33), suggesting that they exert their influence only on substrates present in the bacterium's local environment that have been produced following the onset of inflammation. This contrasts with the inhibitory activity of SLS, which acts at the apical surface of a cell or epithelium and exerts its influence at a distance from its target cells, PMNs, which are primarily located on the basolateral surface of the cell. This is most likely accomplished by interfering with local chemotactic signaling that most likely does not involve IL-8. Thus, all these anti-inflammatory signals may work in concert, with SLS acting to inhibit chemotactic signals produced during the initial streptococcus-host cell interaction and the surface proteases acting subsequently to eliminate signaling molecules that are produced by the host's response to an increasing tissue burden of the replicating pathogen as the infection progresses.

The idea that SLS promotes the ability of *S. pyogenes* to establish a niche in host tissue is consistent with the proposal that SLS was originally a bacteriocin that was subsequently adapted for modulation of host cell behavior (75). This hypothesis is based on the similarity between the structure of the SLS operon and the structures of operons encoding bacteriocins, which are often produced by bacteria to control and out-compete resident flora (20). This capability provides an advantage to a bacterium attempting to establish a niche following its introduction into a naïve host. The SLS operon also encodes a putative immunity protein similar to the proteins encoded by bacteriocin operons (56). These proteins act to protect the producing bacterium from damage caused by its own bacteriocin, which, like SLS, functions by damaging the cell membrane (20). However, unlike SLS, bacteriocins are typically incapable of damaging the membranes of eukaryotic cells (20). There are notable exceptions, including the bacteriocin/cytolysin of *Enterococcus faecalis*, which can damage both bacterial and host cell membranes and does contribute to virulence (13). The process by which SLS may have been adapted from a bacteriocin is not known. However, the observation that several other membrane-active toxins with some similarity to bacteriocins and/or SLS have been found in other pathogens (25, 63) suggests that the adaptation of bacteriocins for host-pathogen interactions may be a common theme.

Another similarity to many bacteriocins is that expression of SLS is subject to a high degree of regulation that is manifested at the level of transcription (27). This is consistent with the idea that *S. pyogenes* may balance the expression of its pro- and anti-inflammatory factors during distinct stages of the infection in order to manipulate the overall magnitude of the host's inflammatory response. Additional support for this has come from the observations that disregulation of virulence factor expression via mutation of several global regulators can significantly enhance streptococcal tissue damage and invasiveness in murine models (16, 21, 34, 45, 68). In a similar vein, the presence of multiple pro- and anti-inflammatory factors may suggest that the same overall balance can be obtained using different combinations of these factors in different strains. The observation that the contribution of SLS to pathogenesis in murine models is often strain specific and influenced by the level of expression of other virulence traits (24, 67) may reflect this notion of overall balance. This model would predict that growth of *S. pyogenes* in tissues that the organism has not evolved to infect may not provide the expected cues for the regulatory program, which could lead to an unbalanced manipulation of the host's response. In turn, this could produce consequences like the sustained dampening of the inflammatory response that has been noted to be associated with poor outcomes for infection of the fascia and muscle (1, 32); this model is also consistent with studies that have established that the rate of bacterial killing is determined by the concentration of neutrophils and not the ratio of neutrophils to bacteria (46). A delay in the recruitment of neutrophils to extravascular sites could allow a small number of bacteria to proliferate to high numbers, causing significant local tissue damage. This is also consistent with our bacterial recovery data, in which growth rates are initially slower in the mutant but subsequently equalize at later time points, suggesting that early on the presence of neutrophils is important to streptococcal clearance but that at later time points other streptococcal virulence factors are involved (e.g., C5a peptidase and DNases that help in evasion

from neutrophils) and make neutrophil presence and bacterial number less pertinent to the progression of the infection. Even at the 6-h time point, the difference in bacterial numbers is not striking, and, again, there is no difference at 12 h, so the growth rate of strains during infection is not likely the main reason for the differences in neutrophil behaviors. Thus, the ability of *S. pyogenes* to balance expression of its pro- and anti-inflammatory factors likely plays a critical role in its ability to cause acute infection.

The strategy of using both pro- and anti-inflammatory factors to manipulate the host's response has been reported for other extracellular pathogens. For example, *Staphylococcus aureus* (48) uses global regulators of transcription, like the Agr quorum-sensing pathway, to balance the expression of factors involved colonization and biofilm formation with the expression of several proinflammatory toxins at different stages of infection, favoring expression of colonization factors at lower cell densities and toxins at higher cell densities (reviewed in reference 9). Similarly, the gram-negative bacterium *Yersinia pestis* progresses from an initial anti-inflammatory state to a highly proinflammatory state within a few days of infection of the lung (42), and this process is dependent on temporal regulation of the plasminogen activator Pla (43). When combined with the data presented here for *S. pyogenes*, these observations suggest that the ability to balance expression of pro- and anti-inflammatory factors in temporally specific patterns may be emerging as a theme for the extracellular pathogens that cause acute infections.

ACKNOWLEDGMENTS

We are indebted to many individuals who generously shared their expertise in zebrafish embryo biology and in microinjection, including J. R. Rawls, Lali Ramakrishnan, and Eric Schroeter. We thank David Hunstad for his assistance in preparing PMNs. We also thank A. Thomas Look for his gift of pu.1-GFP zebrafish. LysM-eGFP mice were a generous gift from Klaus Ley (Robert M. Berne Cardiovascular Research Center, University of Virginia), who backcrossed the originally generated mice from T. Graf (Albert Einstein College of Medicine, Bronx, NY) to the B6 background.

This work was supported by Public Health Service grants AI046433 and AI064721, and A.L. received support from grants K12 HD0473 and K12 HD00850 and institutional training grant T32 HD043010, all from the National Institutes of Health.

REFERENCES

1. **Bakleh, M., L. E. Wold, J. N. Mandrekar, W. S. Harmsen, H. H. Dimashkieh, and L. M. Baddour.** 2005. Correlation of histopathologic findings with clinical outcome in necrotizing fasciitis. Clin. Infect. Dis. **40:**410–414.
2. **Bernheimer, A. W.** 1967. Physical behavior of streptolysin S. J. Bacteriol. **93:**2024–2025.
3. **Betschel, S. D., S. M. Borgia, N. L. Barg, D. E. Low, and J. C. De Azavedo.** 1998. Reduced virulence of group A streptococcal Tn*916* mutants that do not produce streptolysin S. Infect. Immun. **66:**1671–1679.
4. **Boukamp, P., R. T. Petrussevska, D. Breitkreutz, J. Hornun, A. Markham, and N. E. Fusenig.** 1988. Normal keratinization in a spontaneously immortalized aneuploid human keratinocyte one. J. Cell Biol. **106**.
5. **Caparon, M. G., D. S. Stephens, A. Olsen, and J. R. Scott.** 1991. Role of M. protein in adherence of group A streptococci. Infect. Immun. **59:**1811–1817.
6. **Carapetis, J., A. Steer, E. Mulholland, and M. Weber.** 2005. The global burden of streptococcal diseases. Lancet Infect. Dis. **5:**685–694.
7. **Carr, A., D. D. Sledjeski, A. Podbielski, M. D. Boyle, and B. Kreikemeyer.** 2001. Similarities between complement-mediated and streptolysin S-mediated hemolysis. J. Biol. Chem. **276:**41790–41796.
8. **Chen, C. C., and P. P. Cleary.** 1990. Complete nucleotide sequence of the streptococcal C5a peptidase gene of *Streptococcus pyogenes*. J. Biol. Chem. **265:**3161–3167.
9. **Cheung, A. L., A. S. Bayer, G. Zhang, H. Gresham, and Y.-Q. Xiong.** 2004. Regulation of virulence determinants in vitro and in vivo in *Staphylococcus aureus*. FEMS Immunol. Med. Microbiol. **40:**1–9.
10. **Cho, K., and M. G. Caparon.** 2005. Patterns of virulence gene expression differ between biofilm and tissue communities of *Streptococcus pyogenes*. Mol. Microbiol. **57:**1545–1556.
11. **Chtanova, T., M. Schaeffer, S. Han, G. van Dooren, M. Nollman, P. Herzmark, et al.** 2008. Dynamics of neutrophil migration in lymph nodes during infection. Immunity **29:**487–496.
12. **Cleary, P., J. Prabu, J. Dale, D. Wexler, and J. Handley.** 1992. Streptococcal C5a peptidase is a highly specific endopeptidase. Infect. Immun. **60:**5219–5223.
13. **Cox, C. R., P. S. Coburn, and M. Gilmore.** 2005. Enterococcal cytolysin: A novel two component peptide that serves as a bacterial defense against eukaryotic and prokaryotic cells. Curr. Protein Pept. Sci. **6:**77–84.
14. **Cunningham, M. W.** 2000. Pathogenesis of group A streptococcal infections. Clin. Microbiol. Rev. **13:**470–511.
15. **Dale, J. B., E. Y. Chiang, D. L. Hasty, and H. S. Courtney.** 2002. Antibodies against a synthetic peptide of SagA neutralize the cytolytic activity of streptolysin S from group A streptococci. Infect. Immun. **70:**2166–2170.
16. **Dalton, T. L., R. I. Hobb, and J. R. Scott.** 2006. Analysis of the role of CovR and CovS in the dissemination of *Streptococcus pyogenes* in invasive skin disease. Microb. Pathog. **20:**221–227.
17. **Datta, V., S. M. Myskowski, L. A. Kwinn, D. N. Chiem, N. Varki, R. G. Kansai, M. Kotb, and V. Nizet.** 2005. Mutational analysis of group A streptococcal operon encoding streptolysin S and its virulence role in invasive infection. Mol. Microbiol. **56:**681–695.
18. **Davis, J. M., H. Clay, J. L. Lewis, N. Ghori, P. Herbomel, and L. Ramakrishnan.** 2002. Real-time visualization of *Mycobacterium*-macrophage interactions leading to initiation of granuloma formation in zebrafish embryos. Immunity **17:**693–702.
19. **Edwards, R., G. Taylor, M. Ferguson, S. Murray, N. Rendell, A. Wrigley, Z. Bai, J. Boyle, S. Finney, A. Jones, H. Russell, C. Turner, J. Cohen, L. Faulkner, and S. Sriskandan.** 2005. Specific C-terminal cleavage and inactivation of interleukin-8 by invasive disease isolates of *Streptococcus pyogenes*. J. Infect. Dis. **192:**783–790.
20. **Engleberg, N. C., A. Heath, A. Miller, C. Rivera, and V. J. DiRita.** 2001. Spontaneous mutations in the CsrRS two-component regulatory system of *Streptococcus pyogenes* result in enhanced virulence in a murine model of skin and soft tissue infection. J. Infect. Dis. **183:**1043–1054.
21. **Engleberg, N. C., A. Heath, K. Vardaman, and V. J. DiRita.** 2004. Contribution of CsrR-regulated virulence factors to the progress and outcome of murine skin infections by *Streptococcus pyogenes*. Infect. Immun. **72:**623–628.
22. **Faust, N., F. Varas, L. Kelly, S. Heck, and T. Graf.** 2000. Insertion of enhanced green fluorescent protein into the lysozyme gene creates mice with green fluorescent granulocytes and macrophages. Blood **96:**719–726.
23. **Ferretti, J. J., W. M. McShan, D. Adjic, D. Savic, G. Savic, K. Lyon, C. Primeaux, S. S. Sezate, A. N. Surorov, S. Kenton, H. Lai, S. Lin, Y. Qian, H. G. Jia, F. Z. Najar, Q. Ren, H. Zhu, L. Song, J. White, X. Yuan, S. W. Clifton, B. A. Rose, and R. E. McLaughlin.** 2001. Complete genome sequence of an M1 strain of *Streptococcus pyogenes*. Proc. Natl. Acad. Sci. USA **98:**4658–4663.
24. **Fontaine, M. C., J. J. Lee, and M. A. Kehoe.** 2003. Combined contributions of streptolysin O and streptolysin S to virulence of serotype M5 *Streptococcus pyogenes* strain Manfredo. Infect. Immun. **71:**3857–3865.
25. **Fuller, J. D., A. C. Camus, C. L. Duncan, V. Nizet, D. J. Bast, R. L. Thune, D. E. Low, and J. C. De Azavedo.** 2002. Identification of a streptolysin S-associated gene cluster and its role in the pathogenesis of *Streptococcus iniae* disease. Infect. Immun. **70:**5730–5739.
26. **Galdiero, M., M. Vitiello, P. Scarfogliero, and L. Sommese.** 1997. Growth hormone release of interleukin-1 alpha, interferon-gamma and interleukin-4 from murine splenocytes stimulated with staphylococcal protein A, toxic shock syndrome toxin-1 and streptococcal lysin S. Eur. Cytokine Netw. **8:**83–90.
27. **Gao, J., A. A. Gusa, J. R. Scott, and G. Churchward.** 2005. Binding of the global response regulator CovR to SagA of *Streptococcus pyogenes* reveals a new mode of CovR-DNA interaction. J. Biol. Chem. **280:**38948–38956.
28. **Ginsburg, I.** 1999. Is streptolysin S of group A streptococci a virulence factor? APMIS **107:**1051–1059.
29. **Ginsburg, I.** 1970. Streptolysin S, p. 100–171. *In* T. C. Montie, S. Kadis, and S. J. Ajl (ed.), Microbial toxins, vol. 3. Academic Press, New York, NY.
30. **Hanski, E., and M. G. Caparon.** 1992. Protein F, a fibronectin-binding protein, is an adhesin of the group A streptococcus, *Streptococcus pyogenes*. Proc. Natl. Acad. Sci. USA **89:**6172–6176.
31. **Herbomel, P., B. Thisse, and C. Thisse.** 1999. Ontogeny and behaviour of early macrophages in the zebrafish embryo. Development **126:**3735–3745.
32. **Hidalgo-Grass, C., M. Dan-Goor, A. Maly, Y. Eran, L. Kwinn, V. Nizet, M. Ravins, J. Jaffe, A. Peyser, A. Moses, and E. Hanski.** 2004. Effect of a bacterial pheromone peptide on host chemokine degradation in group A streptococcal necrotising soft-tissue infections. Lancet **363:**696–703.
33. **Hidalgo-Grass, C., I. Mishalian, M. Dan-Goor, I. Belotserkovsky, Y. Eran, V. Nizet, A. Peled, and E. Hanski.** 2006. A streptococcal protease that degrades CXC chemokines and impairs bacterial clearance from infected tissues. EMBO J. **25:**4628–4637.
34. **Hidalgo-Grass, C., M. Ravins, M. Dan-Goor, J. Jaffe, A. Moses, and E.**

Hanski. 2002. A locus of group A streptococcus involved in invasive disease and DNA transfer. Mol. Microbiol. **46:**87–99.
35. **Hirsch, J. G., A. W. Bernheimer, and G. Weissman.** 1963. Motion picture study of the toxic action of streptolysins on leukocytes. J. Exp. Med. **118:** 223–228.
36. **Hsu, K., D. Traver, J. L. Kutok, A. Hagen, T. X. Liu, B. H. Paw, J. Rhodes, J. Berman, L. I. Zon, J. P. Kanki, and A. T. Look.** 2004. The pu.1 promoter drives myeloid gene expression in zebrafish. Blood **104:**1291–1297.
37. **Jault, C., L. Pichon, and J. Chluba.** 2004. Toll-like receptor gene family and TIR-domain adapters in *Danio rerio*. Mol. Immunol. **40:**759–771.
38. **Ji, Y., L. McLandsborough, A. Kondagunta, and P. P. Cleary.** 1996. C5a peptidase alters clearance and trafficking of group A streptococci by infected mice. Infect. Immun. **64:**503–510.
39. **Kimmel, C., W. Ballard, S. Kimmel, B. Ullmann, and S. T. F.** 1995. Stages of embryonic development of the zebrafish. Dev. Dynamics **203:**253–310.
40. **Klein, C., E. Medina, L. Sander, U. Dierssen, T. Roskams, W. Mueller, C. Trautwein, and O. Goldmann.** 2007. Contribution of interleukin-6/gp130 signaling in hepatocytes to the inflammatory response in mice infected with *Streptococcus pyogenes*. J. Infect. Dis. **196:**755–762.
41. **Kushner, S. R.** 1978. An improved method for transformation of *Escherichia coli* with ColE1-derived plasmids. Elsevier-North Holland Biomedical Press, New York, NY.
42. **Lathem, W., S. Crosby, V. Miller, and W. Goldman.** 2005. Progression of primary pneumonic plague: A mouse model of infection, pathology, and bacterial transcriptional activity. Proc. Natl. Acad. Sci. USA **102:**17786–17791.
43. **Lathem, W., P. Price, V. Miller, and W. Goldman.** 2007. A plasminogen-activating protease specifically controls the development of primary pneumonic plague. Science **315:**509–513.
44. **Lee, S., D. Mitchell, A. Markley, M. Hensler, D. Gonzalez, A. Wohlrab, P. Dorrestein, V. Nizet, and J. Dixon.** 2008. Discovery of a widely distributed toxin biosynthetic gene cluster. Proc. Natl. Acad. Sci. USA **105:**5879–5884.
45. **Levin, J. C., and M. R. Wessels.** 1998. Identification of csrR/csrS, a genetic locus that regulates hyaluronic capsule synthesis in group A streptococcus. Mol. Microbiol. **30:**209–219.
46. **Li, Y., A. Karlin, J. Loike, and S. Silverstein.** 2002. A critical concentration of neutrophils is required for effective bacterial killing in suspension. Proc. Natl. Acad. Sci. USA **99:**8289–8294.
47. **Lipschutz, J. H., Y. A. Lucy, E. O'Brien, Y. Altschuler, D. Avrahani, Y. Nguyen, K. Tang, and K. E. Mostov.** 2001. Analysis of membrane traffic in polarized epithelial cells, p. 15.15.11–15.15.18. *In* J. S. Bonifacino, M. Dasso, J. B. Harford, J. Lippincott-Schwartz, and K. M. Yamada (ed.), Current protocols in cell biology. John Wiley and Sons, Inc., Hoboken, NJ.
48. **Lyon, G. J., and R. P. Novick.** 2004. Peptide signaling in Staphylococcus aureus and other gram-positive bacteria. Peptides **25:**1389–1403.
49. **Lyon, W. R., J. C. Madden, J. C. Levin, J. L. Stein, and M. G. Caparon.** 2001. Mutation of *luxS* affects growth and virulence factor expression in *Streptococcus pyogenes*. Mol. Microbiol. **42:**145–157.
50. **Mathias, J. R., B. J. Perrin, T.-X. Liu, J. P. Kanki, A. T. Look, and A. Huttenlocher.** 2006. Resolution of inflammation by retrograde chemotaxis of neutrophils in trangenic zebrafish. J. Leukoc. Biol. **80:**1281–1288.
51. **McCormick, B. A.** 2003. The use of transepithelial models to examine host-pathogen interactions. Curr. Opin. Microbiol. **6:**77–81.
52. **Meijer, A. H., S. F. G. Krens, I. A. Medina Rodriguez, S. He, W. Bitter, E. Snaar-Jagalska, and H. P. Spaink.** 2004. Expression analysis of the Toll-like receptor and TIR domain adaptor families of zebrafish. Mol. Immunol. **40:**773–783.
53. **Miyoshi-Akiyama, T., D. Takamatsu, M. Koyanagi, J. Zhao, K. Imanishi, and T. Uchiyama.** 2005. Cytocidal effect of *Streptococcus pyogenes* on mouse neutrophils in vivo and the critical role of streptolysin S. J. Infect. Dis. **192:**107–116.
54. **Neely, M. N., J. D. Pfeifer, and M. G. Caparon.** 2002. A streptococcal-zebrafish model of bacterial pathogenesis. Infect. Immun. **70:**3904–3914.
55. **Nizet, V.** 2002. Streptococcal b-hemolysins: genetics and role in disease pathogenesis. Trends Microbiol. **10:**575–579.
56. **Nizet, V., B. Beall, D. J. Bast, V. Datta, L. Kilburn, D. E. Low, and J. C. De Azavedo.** 2000. Genetic locus for streptolysin S production by group A streptococcus. Infect. Immun. **68:**4245–4254.
57. **Ofek, I., S. Bergner-Rabinowitz, and I. Ginsburg.** 1972. Oxygen-stable hemolysins of group A streptococci VIII. Leukotoxic and antiphagocytic effects of streptolysins S and O. Infect. Immun. **6:**459–464.
58. **Ofek, I., D. Zafriri, J. Goldhar, and B. Eisenstein.** 1990. Inability of toxin inhibitors to neutralize enhanced toxicity caused by bacteria adherent to tissue culture cells. Infect. Immun. **58:**3737–3742.
59. **Okada, N., A. Pentland, P. Falk, and M. G. Caparon.** 1994. M protein and protein F act as important determinants of cell-specific tropism of *Streptococcus pyogenes* in skin tissue. J. Clin. Investig. **94:**965–977.
60. **Pahlman, L. I., M. Morgelin, J. Eckert, L. Johansson, W. Russell, K. Riesbeck, O. Soehnlein, L. Lindbom, A. Norrby-Teglund, and R. R. Schumann.** 2006. Streptococcal M protein: a multipotent and powerful inducer of inflammation. J. Immunol. **177:**1221–1228.
61. **Parkos, C. A., C. Delp, M. A. Arnout, and J. Madara.** 1991. Neutrophil migration across a cultured intestinal epithelium: dependence on a CD11b/CD18-mediated event and enhanced efficiency of physiologic direction. J. Clin. Investig. **88:**1605–1612.
62. **Peters, N., J. Egen, N. Secundino, A. Debrabant, N. Kimblin, S. Kamhawi, et al.** 2008. In vivo imaging reveals an essential role for neutrophils in leishmaniasis transmitted by sand flies. Science **321:**970–974.
63. **Pritzlaff, C. A., J. C. Chang, G. S. Tamura, C. E. Rubens, and V. Nizet.** 2001. Genetic basis for the beta-hemolytic/cytolytic activity of group B streptococcus. Mol. Microbiol. **39:**236–247.
64. **Renshaw, S., C. Loynes, D. Trushell, S. Elworthy, P. Ingham, and M. Whyte.** 2006. A transgenic zebrafish model of neutrophilic inflammation. Blood **108:**3976–3978.
65. **Ruiz, N., B. Wang, A. Pentland, and M. G. Caparon.** 1998. Streptolysin O and adherence synergistically modulate proinflammatory responses of keratinocytes to group A streptococci. Mol. Microbiol. **27:**337–346.
66. **Scott, J. R., P. C. Guenther, L. M. Malone, and V. A. Fischetti.** 1986. Conversion of an M^- group A streptococcus to M^+ by transfer of a plasmid containing M6 gene. J. Exp. Med. **164:**1641–1651.
67. **Sierig, G., C. Cywes, M. R. Wessels, and C. D. Ashbaugh.** 2003. Cytotoxic effects of streptolysin O and streptolysin S enhance the virulence of poorly encapsulated group a streptococci. Infect. Immun. **71:**446–455.
68. **Sumby, P., A. R. Whitney, E. A. Graviss, F. R. DeLeo, and J. M. Musser.** 2006. Genome-wide analysis of group A streptococci reveals a mutation that modulates global phenotype and disease specificity. PLoS Pathog. **2:**41–49.
69. **Swaim, L., L. Connolly, H. Volkman, O. Humbert, D. Born, and L. Ramakrishnan.** 2006. *Mycobacterium marinum* infection of adult zebrafish causes caseating granulomatous tuberculosis and is moderated by adaptive immunity. Infect. Immun. **74:**6108–6117.
70. Reference deleted.
71. **Van der Sar, A. M., R. J. P. Musters, F. J. M. van Eeden, B. J. Appelmelk, C. M. J. E. Vandenbroucke-Grauls, and W. Bitter.** 2003. Zebrafish embryos as a model host for the real time analysis of *Salmonella typhimurium* infections. Cell Micro. **5:**601–611.
72. **Van der Sar, A. M., O. W. Stockhammer, C. van der Laan, H. P. Spaink, W. Bitter, and A. H. Meijer.** 2006. MyD88 innate immune function in a zebrafish embryo infection model. Infect. Immun. **74:**2436–2441.
73. **Wang, B., N. Ruiz, A. Pentland, and M. G. Caparon.** 1997. Keratinocyte proinflammatory responses to adherent and nonadherent group A streptococci. Infect. Immun. **65:**2119–2126.
74. **Ward, A. C., D. O. McPhee, M. M. Condron, S. Varma, S. H. Cody, S. M. N. Onnebo, B. H. Paw, L. I. Zon, and G. J. Lieschke.** 2003. The zebrafish spi1 promoter drives myeloid specific expression in stable transgenic fish. Blood **102:**3238–3240.
75. **Wessels, M. R.** 2005. Streptolysin S. J. Infect. Dis. **192:**13–15.
76. **Westerfield, M.** 2000. The zebrafish book: a guide for laboratory use of zebrafish, *Brachydanio rerio*, 3rd ed. University of Oregon Press, Eugene, OR.
77. **Zinselmeyer, B., J. Dempster, A. Gurney, D. Wokosin, M. Miller, and E. A. Ho.** 2005. In situ characterization of $CD4^+$ behavior in mucosal and systemic lymphoid tissues during the induction of oral priming and tolerance. J. Exp. Med. **201:**1815–1823.
78. **Zinselmeyer, B., J. Lynch, X. Zhang, T. Aoshi, and M. Miller.** 2008. Video-rate two-photon imaging of mouse footpad—a promising model for studying leukocyte recruitment dynamics during inflammation. Inflamm. Res. **57:**93–96.

Editor: A. Camilli